International Journal of Applied Mathematics

Volume 38 No. 5s, 2025

ISSN: 1311-1728 (printed version); ISSN: 1314-8060 (on-line version)

ANALYSIS OF THE STABILITY OF SEMICONDUCTOR QUANTUM DOT LASERS UNDER OPTOELECTRONIC FEEDBACK

Tareq A. Al Attabi[1,2], Muwaffaq Abdullah[2], Salam Jasim Majeed[3]

[1]Department of Physics, College of Sciences, University of Thi-Qar, Thi-Qar, Iraq

[2]University of Sumer, Rifai 66001, Iraq

[3]Department of Mathematics, College of Computer Science and Mathematics, University of Thi-Qar, Thi-Qar, Iraq

Tarqabdalghany@gmail.com, tareq.abdulghane@utq.edu.iq

Mowaffaq_2phy@sci.utq.edu.iq

sjmajeed@utq.edu.iq

Abstract

Studying the dynamics of semiconductor lasers (SLs) is crucial for advancing a wide range of optical technologies. SLs exhibit rich dynamical phenomena, and these behaviors can be harnessed for many novel applications. The dynamical behavior of quantum dot (QD) SLs with optoelectronic feedback (OEFB) have been studied theoretically. After a series of mathematical operations, they were converted into dimensionless equations. Further, after analysis these equations analytically. The results show if the values of $(k, \delta_\circ)$ are positive, the model contains two equilibrium points (boundary $\in^0$, interior $\in^1$). The stability of interior equilibrium is discuss. Moreover the non-delayed system is generalized by adding the feed time delay. The analysis of the generalized model (delayed model), show that the stability of the point $\in^1$ is affected by the value of τ_d. Further the trajectories of the system solutions take periodic paths, where the system has a bifurcation of the Hopf type or a limit cycle affected by the value of τ_d.

Keyword SLs, QD, OEFB, dynamics, equilibrium points, Hopf bifurcation.

Introduction

Studying the behavior and dynamics of a laser system through rate equations is crucial for several reasons to understand laser dynamics. Rate equations help in understanding how populations of various energy levels change over time under the influence of pumping and laser radiation. This understanding is essential for optimizing laser performance and stability. By solving rate equations for laser behavior, researchers can predict the transient and steady-state behavior of lasers. This includes phenomena like threshold behavior, relaxation oscillations, and the evolution of photon number in the laser cavity [1, 2]. Rate equations provide insights into the minimum pumping rate required to achieve population inversion, which is necessary for laser action. This helps in designing lasers that are more efficient and effective for various applications [3]. The equations can be used to determine the optimal output coupling for

Received: August 07 2025

Volume 38 No. 5s, 2025

ISSN: 1311-1728 (printed version); ISSN: 1314-8060 (on-line version)

maximizing the output power of a laser. This is particularly important for applications requiring high-intensity laser beams [4].

Studying the stability and bifurcation of a laser system helps us to understand stability and helps predict how a laser will respond to changes in parameters such as pump power, cavity losses, and external feedback. This is essential for designing stable laser systems that perform reliably under various conditions. By analyzing bifurcations, researchers can identify critical points where the laser's behavior changes dramatically [5, 6]. This knowledge allows for the optimization of laser parameters to achieve desired performance, such as higher output power or specific wavelength emission. Stability analysis helps identify and avoid undesirable behaviors like chaos or mode hopping, which can degrade laser performance [7, 8]. By understanding these dynamics, engineers can design control strategies to mitigate such effects. Rate equations provide a framework for developing control mechanisms to stabilize lasers and maintain their operation within desired regimes. This is particularly important for applications requiring precise and stable laser output [9].

Theoretical model

In the rate equations system, a term is added to the pumping to represent the OEFB effect. In the QDL system, the electrons are first pumped into WL before being collected by the QDs. The dynamics of the occupation probability of carriers in the QD ground state and excited state, where is (N_{wl})the number of carriers in the WL, and the number of photons in the optical mode S are described by the rate equations shown below [10]:

$$S^{\bullet} = -\gamma S + v_g(2\rho - 1)S$$

$$\rho_{gs}^{\bullet} = \gamma_{c_{es}}\rho_{es}(1-\rho_{gs}) - \gamma_d\rho_{gs} - g_o(2\rho_{gs}-1)S$$

$$\rho_{es}^{\bullet} = \gamma_{c_{wl}}N_{wl}(1-\rho_{es}) - \gamma_d\rho_{es} - \gamma_{c_{es}}\rho_{es}(1-\rho_{gs})$$

$$N_{wl}^{\bullet} = \frac{J}{e} - \gamma_n N_{wl} - 2\gamma_{c_{wl}}N_{wl}(1-\rho_{es}) \qquad (1)$$

Where (ρ_{gs}) and (ρ_{es}) are the probability of occupation in a ground and exited states in the QDs, (γ_d) and (γ_n) are the non-radiative decay rates for carriers in the dot and WL respectively, ($\gamma_{c_{wl}}$) and ($\gamma_{c_{es}}$) are the capture rate from wetting layer into an empty exited state and from exited into ground states respectively. (J) is the electrically injection pump current per dot, (e) is elementary charge. The last terms in Eq. (3) and Eq.(4) describe the rate of exchange of carriers between a ground state and exited state in the dots and between the well and the exited state in the dots. For analytical and numerical purpose, it is useful to rewrite Eqs.(1,2,3,4) in dimensionless form, to this end we introduce the new variables [94]: $x = \frac{g_o}{\gamma_d}S$, $u = \frac{vg_o}{\gamma_s}(2\rho_{gs}-1)$, $z = \rho_{es}$, $w = \frac{\gamma_{c_{wl}}}{vg_o}N_{wl}$, $\Gamma = \frac{\gamma_{c_{es}}}{\gamma_s}$, $\Gamma_1 = \frac{vg_o}{\gamma_s}$, $\Gamma_2 = \frac{\gamma_d}{\gamma_s}$, $\Gamma_3 = \frac{\gamma_{c_{wl}}}{\gamma_s}$, $\Gamma_4 = \frac{\gamma_n}{\gamma_s}$, $\delta_o = \frac{J}{g_o ve}$ and the time scale $t'^0 = \gamma_s t$.

Received: August 07 2025

International Journal of Applied Mathematics

Volume 38 No. 5s, 2025

ISSN: 1311-1728 (printed version); ISSN: 1314-8060 (on-line version)

The rate equations then become as following:

$$\begin{aligned}
\dot{x} &= x(y-1),\\
\dot{y} &= \Gamma z(\Gamma_1 - y)) - \Gamma_2 y(1+2x) - \Gamma_1\Gamma_2,\\
\dot{z} &= \Gamma_1 w(1-z) - \Gamma_2 z - \tfrac{1}{2}\Gamma z\left(1-\tfrac{y}{\Gamma_1}\right),\\
\dot{w} &= \delta_0\,\Gamma_3(1-\tfrac{kx}{x_0}) - \Gamma_4 w - 2w(1-z)\Gamma_3.
\end{aligned} \tag{2}$$

Equilibrium of Non-delayed Model (2)

In this section, we investigate the existence of the equilibrium points of the system (2). To do that the following equations must be solve:

$$\begin{aligned}
x(y-1) &= 0,\\
\Gamma z(\Gamma_1 - y)) - \Gamma_2 y(1+2x) - \Gamma_1\Gamma_2 &= 0,\\
\Gamma_1 w(1-z) - \Gamma_2 z - \frac{1}{2}\Gamma z\left(1-\frac{y}{\Gamma_1}\right) &= 0,\\
\delta_0\,\Gamma_3(1-\frac{kx}{x_0}) - \Gamma_4 w - 2w(1-z)\Gamma_3 &= 0.
\end{aligned}$$

From solving the first equation of the above system we have two cases and then fixed points of system (2).

Therefore the system has the boundary equilibrium point when $x = 0$, and the interior equilibrium point when $y = 1$.

Case one: use $x = 0$, the above system of algebraic equations reduced to :

$$\begin{aligned}
\Gamma z(\Gamma_1 - y)) - \Gamma_2 y - \Gamma_1\Gamma_2 &= 0,\\
\Gamma_1 w(1-z) - \Gamma_2 z - \frac{1}{2}\Gamma z\left(1-\frac{y}{\Gamma_1}\right) &= 0,\\
\delta_0\,\Gamma_3 - \Gamma_4 w - 2w(1-z)\Gamma_3 &= 0.
\end{aligned}$$

Solve first equation gives that:

$$y = \frac{\Gamma_1(\Gamma z - \Gamma_2)}{\Gamma z + \Gamma_2}$$

While third equation gives:

$$w = \frac{\delta_0\,\Gamma_3}{\Gamma_4 + 2(1-z)\Gamma_3}$$

y and w are positives if

$$\frac{\Gamma_2}{\Gamma} < z \leq 1\,.$$

Received: August 07 2025

International Journal of Applied Mathematics

Volume 38 No. 5s, 2025

ISSN: 1311-1728 (printed version); ISSN: 1314-8060 (on-line version)

Apply y and w in second equation gives

$$Az^3 + Bz^2 + Cz + D = 0,$$

where,

$A = 4\delta_0\Gamma_1{\Gamma_3}^2\Gamma > 0,$

$B = -(2S_0\Gamma\Gamma_1\Gamma_3\Gamma_4 + 8S_0\Gamma\Gamma_1\Gamma_3^2 - 4S_0\Gamma_1\Gamma_2\Gamma_3^2 + 4\Gamma\Gamma_2\Gamma_3 + 4\Gamma_2^2\Gamma_3 + 2\Gamma\Gamma_3),$

$C = 2S_0\Gamma\Gamma_1\Gamma_3\Gamma_4 - 2S_0\Gamma_1\Gamma_2\Gamma_3\Gamma_4 + 4S_0\Gamma\Gamma_1\Gamma_3^2 - 8S_0\Gamma_1\Gamma_2\Gamma_3^2 + 2\Gamma_2^2\Gamma_4 - 2\Gamma\Gamma_2\Gamma_4 + 4\Gamma\Gamma_2\Gamma_3 + 4\Gamma_2^2\Gamma_3 - \Gamma\Gamma_4 + 2\Gamma\Gamma_3,$

$D = 2S_0\Gamma_1\Gamma_2\Gamma_3\Gamma_4 + 4S_0\Gamma_1\Gamma_2\Gamma_3^2 > 0.$

Here z is the positive root of the last equation, this may be gain if :

$B < 0,$ or $C < 0.$

Therefore, we can say the system has the boundary equilibrium point $\in^{\circ} = (0, y, z, w).$

Case two: use $y = 1$, system (2) reduced to :

$$\begin{aligned}
\Gamma z(\Gamma_1 - 1)) - \Gamma_2(1 + 2x) - \Gamma_1\Gamma_2 \quad &= 0,\\
\Gamma_1 w(1 - z) - \Gamma_2 z - \frac{1}{2}\Gamma z\left(1 - \frac{1}{\Gamma_1}\right) \quad &= 0,\\
\delta_0\,\Gamma_3(1 - \frac{kx}{x_0}) - \Gamma_4 w - 2w(1 - z)\Gamma_3 \quad &= 0.
\end{aligned}$$

From first equation one can have

$$x = \Gamma_5 z - \Gamma_6,$$

where,

$\Gamma_5 = \dfrac{\Gamma(\Gamma_1 - 1)}{2\Gamma_2},$

$\Gamma_6 = (1 + \Gamma_1)/2,$

and x is positive if

$\Gamma_1 > 1$ and z $> \frac{\Gamma_6}{\Gamma_5}.$

Further from second equation can get

$$w = \Gamma_7\frac{z}{1 - z},$$

Where, $\Gamma_7 = \frac{\Gamma_2 + \frac{\Gamma}{2} + \frac{\Gamma}{2\Gamma_1}}{\Gamma_1}$. Here, w is positive if

$0 < z < 1.$

Now use x and w formulas in third equation with some computation can have

Received: August 07 2025

International Journal of Applied Mathematics

Volume 38 No. 5s, 2025

ISSN: 1311-1728 (printed version); ISSN: 1314-8060 (on-line version)

$$\mathrm{A}z^2 + \mathrm{B}z + \mathrm{C} = 0, \qquad (3)$$

where,

$A = (\mathrm{S_o K}\Gamma_1\Gamma_3\Gamma + 2\mathrm{x}_0\Gamma_2\Gamma_3\Gamma)(\Gamma_1 - 1),$

$\mathrm{B} = 2\mathrm{x}_0\Gamma_1\Gamma_2\mathrm{S_o}\Gamma_3 + \mathrm{S_o K}{\Gamma_1}^2\Gamma_3\Gamma - \mathrm{S_o K}\Gamma_1\Gamma_3\Gamma + \mathrm{S_o K}\Gamma_1\Gamma_3\Gamma_2 + \mathrm{S_o K}{\Gamma_1}^2\Gamma_3\Gamma_2$

$\quad + 2\mathrm{x}_0\Gamma_2^2\Gamma_4 + \mathrm{x}_0\Gamma_2\Gamma_4\Gamma + \frac{\mathrm{x}_0\Gamma_2\Gamma_4\Gamma}{\Gamma_1} + 2\mathrm{x}_0\Gamma_2\Gamma_1\Gamma\Gamma_3 - 2\mathrm{x}_0\Gamma_2\Gamma\Gamma_3,$

$\mathrm{C} = 2\mathrm{x}_0\Gamma_1\Gamma_2\mathrm{S_o}\Gamma_3 + \mathrm{S_o K}\Gamma_1\Gamma_3\Gamma_2 + \mathrm{S_o K}{\Gamma_1}^2\Gamma_3.$

and z is the positive root of equation (3). Therefore we have the interior equilibrium point of system (2) as $\in^1 = (x, 1, w, z)$.

Stability Analysis of the Equilibrium $\in^1$ of Model (2)

The main approach in this section is the analysis of nonlinear dynamical system (2) near the point $\in^1$. The Jacobian linearization technique is used to find the local model that is linear in the state variables x and y.

Non-delayed System (2) at any point (x, y, z, w) has the next Jacobian matrix

$$N(x, y, z, w) = \begin{pmatrix} y-1 & x & 0 & 0 \\ -2\Gamma_2 y & -\Gamma \mathrm{z} - \Gamma_2 - 2\Gamma_2 x & \Gamma(\Gamma_1 - \mathrm{y}) & 0 \\ 0 & \frac{\Gamma \mathrm{z}}{2\Gamma_1} & -\Gamma \mathrm{w} - \Gamma_2 - \frac{\Gamma}{2} + \frac{\Gamma \mathrm{y}}{2\Gamma_1} & \Gamma_1(1-\mathrm{z}) \\ \frac{\mathrm{S_o}\Gamma_3 k}{x_0} & 0 & 2\Gamma_3 w & -\Gamma_4 - 2\Gamma_3(1-\mathrm{z}) \end{pmatrix}$$

This matrix, when $(x, y, z, w) = (x^1, 1, z^1, w^1)$, reduced to

$$N^1 = N(\in^1)$$

$$= \begin{pmatrix} 0 & x^1 & 0 & 0 \\ -2\Gamma_2 & -\Gamma z^1 - \Gamma_2 - 2\Gamma_2 x^1 & \Gamma(\Gamma_1 - 1) & 0 \\ 0 & \frac{\Gamma z^1}{2\Gamma_1} & -\Gamma w^1 - \Gamma_2 - \frac{\Gamma}{2} + \frac{\Gamma}{2\Gamma_1} & \Gamma_1(1 - z^1) \\ \frac{\mathrm{S_o}\Gamma_3 k}{x_0} & 0 & 2\Gamma_3 w^1 & -\Gamma_4 - 2\Gamma_3(1 - z^1) \end{pmatrix}$$

. (4)

The characteristic equation of N^1 is given by

$$|N^1 - \lambda \mathrm{I}| = 0,$$

or

Received: August 07 2025

Volume 38 No. 5s, 2025

ISSN: 1311-1728 (printed version); ISSN: 1314-8060 (on-line version)

$$\begin{vmatrix} -\lambda & x^1 & 0 & 0 \\ -2\Gamma_2 & -\Gamma z^1-\Gamma_2-2\Gamma_2 x^1-\lambda & \Gamma(\Gamma_1-1) & 0 \\ 0 & \dfrac{\Gamma z^1}{2\Gamma_1} & -\Gamma w^1-\Gamma_2-\dfrac{\Gamma}{2}+\dfrac{\Gamma}{2\Gamma_1}-\lambda & \Gamma_1(1-z^1) \\ \dfrac{\mathrm{S_o}\Gamma_3 k}{x_0} & 0 & 2\Gamma_3 w^1 & -\Gamma_4-2\Gamma_3(1-z^1)-\lambda \end{vmatrix}=0.$$

The last equation gives

$$(-\lambda)\begin{vmatrix} -\Gamma z^1-\Gamma_2-2\Gamma_2 x^1-\lambda & \Gamma(\Gamma_1-1) & 0 \\ \dfrac{\Gamma z^1}{2\Gamma_1} & -\Gamma w^1-\Gamma_2-\dfrac{\Gamma}{2}+\dfrac{\Gamma}{2\Gamma_1}-\lambda & \Gamma_1(1-z^1) \\ 0 & 2\Gamma_3 w^1 & -\Gamma_4-2\Gamma_3(1-z^1)-\lambda \end{vmatrix}$$

$$-(x^1)\begin{vmatrix} -2\Gamma_2 & \Gamma(\Gamma_1-1) & 0 \\ 0 & -\Gamma w^1-\Gamma_2-\dfrac{\Gamma}{2}+\dfrac{\Gamma}{2\Gamma_1}-\lambda & \Gamma_1(1-z^1) \\ \dfrac{\mathrm{S_o}\Gamma_3 k}{x_0} & 2\Gamma_3 w^1 & -\Gamma_4-2\Gamma_3(1-z^1)-\lambda \end{vmatrix}=0,$$

With some computation the above equation can be written in the next polynomial form

$$\lambda^4+A_1\lambda^3+B_1\lambda^2+C_1\lambda+D_1=0, \qquad (5)$$

where,

$$A_1=2\Gamma_2\Gamma_5 z-2\Gamma_2\Gamma_6+\Gamma\Gamma_7\frac{\mathrm{z}}{1-\mathrm{z}}+\Gamma_2+\frac{\Gamma}{2}-\frac{\Gamma\Gamma_5\mathrm{z}-\Gamma\Gamma_6}{2\Gamma_1}+\Gamma_4+$$

Received: August 07 2025

Volume 38 No. 5s, 2025

ISSN: 1311-1728 (printed version); ISSN: 1314-8060 (on-line version)

$$
\begin{aligned}
(1-z)\,,B_1 = {} & \Gamma^2\Gamma_7\frac{Z^2}{1-Z} + \Gamma\Gamma_2 z + \frac{\Gamma^2 z}{2} - \frac{\Gamma^2\Gamma_5 z^2 - \Gamma^2\Gamma_6 z}{2\Gamma_1} + \Gamma\Gamma_4 z + 2\Gamma\Gamma_3(1-z) \\
& + \Gamma\Gamma_2\Gamma_7\frac{z}{1-z} + \Gamma_2{}^2 + \frac{\Gamma\Gamma_2}{2} - \frac{\Gamma\Gamma_2\Gamma_5 z - \Gamma\Gamma_2\Gamma_6}{2\Gamma_1} + 2\Gamma_2\Gamma_4 + 2\Gamma_2\Gamma_3(1-z) \\
& + 2\Gamma\Gamma_2\Gamma_5\Gamma_7\frac{z^2}{1-z} + \Gamma^2\Gamma_5 z + \Gamma\Gamma_2\Gamma_5 z - \frac{\Gamma_2\Gamma_5{}^2\Gamma z - \Gamma_2\Gamma_5\Gamma\Gamma_6 z}{\Gamma_1} + 2\Gamma_2\Gamma_5\Gamma_4 z \\
& - 2\Gamma_2\Gamma_6\Gamma\Gamma_7\frac{z}{1-z} - 2\Gamma_2{}^2\Gamma_6 - \Gamma_2\Gamma_6\Gamma + \frac{\Gamma_2\Gamma_6{}^2\Gamma z - \Gamma_2\Gamma_6{}^2\Gamma}{\Gamma_1} - 2\Gamma_2\Gamma_6\Gamma_4 \\
& - 4\Gamma_2\Gamma_6\Gamma_3(1-z) + \Gamma\Gamma_7\Gamma_4\frac{z}{1-z} + 2\Gamma\Gamma_7\Gamma_3 z + 2\Gamma_2\Gamma_3(1-z) + \frac{\Gamma\Gamma_4}{2} \\
& + \Gamma\Gamma_3(1-z) + \frac{\Gamma_4\Gamma\Gamma_5 z - \Gamma_4\Gamma\Gamma_6}{2\Gamma_1} - \frac{\Gamma_3\Gamma\Gamma_5 z - \Gamma_3\Gamma\Gamma_6}{\Gamma_1}(1-z) - 2\Gamma_1\Gamma_3\Gamma_7 z \\
& - 2\Gamma_2\Gamma_5 z + 2\Gamma_2\Gamma_6, \quad C_1 \\
& = \Gamma^2\Gamma\Gamma_7\frac{z^2}{1-z} + 2\Gamma^2\Gamma_3\Gamma_7 z^2 + \Gamma\Gamma_2\Gamma_4 z + 2\Gamma\Gamma_2\Gamma_3 z(1-z) + \frac{\Gamma^2\Gamma_4 z}{2} \\
& + \Gamma^2\Gamma_3 z(1-z) - \frac{\Gamma_4\Gamma^2\Gamma_5 z^2 - \Gamma^2\Gamma_4\Gamma_6 z}{2\Gamma_1} - \frac{\Gamma^2\Gamma_3\Gamma_5 Z^2 - \Gamma^2\Gamma_3\Gamma_6 Z}{\Gamma_1}(1-Z) \\
& + \Gamma\Gamma_2\Gamma_4\Gamma_7\frac{Z}{1-Z} + 2\Gamma\Gamma_2\Gamma_3\Gamma_7 Z + \Gamma_2{}^2\Gamma_4 + 2\Gamma_2{}^2\Gamma_3(1-Z) + \frac{\Gamma\Gamma_2\Gamma_4}{2} \\
& + \Gamma\Gamma_2\Gamma_3(1-Z) - \frac{\Gamma\Gamma_2\Gamma_4\Gamma_5 Z - \Gamma\Gamma_2\Gamma_4\Gamma_6}{2\Gamma_1} - \frac{\Gamma\Gamma_2\Gamma_3\Gamma_5 Z - \Gamma\Gamma_2\Gamma_3\Gamma_6}{2\Gamma_1}(1-Z) \\
& - 2\Gamma_1\Gamma_2\Gamma_3\Gamma_7 Z + 2\Gamma\Gamma_2\Gamma_4\Gamma_5\Gamma_7\frac{Z^2}{1-Z} + 4\Gamma\Gamma_2\Gamma_3\Gamma_7 Z^2 + 2\Gamma_2{}^2\Gamma_5\Gamma_4 Z \\
& + 4\Gamma_2{}^2\Gamma_5\Gamma_3 Z(1-Z) + \Gamma\Gamma_2\Gamma_5\Gamma_4 Z + 2\Gamma\Gamma_2\Gamma_3\Gamma_5 Z(1-Z) \\
& - \frac{\Gamma^2\Gamma\Gamma_5{}^2\Gamma_4 Z^2 - \Gamma\Gamma_2\Gamma_4\Gamma_5\Gamma_6 Z}{\Gamma_1} - \frac{2\,\Gamma_2\Gamma\Gamma_5{}^2\Gamma_3 Z^2 - 2\Gamma\Gamma_2\Gamma_3\Gamma_5\Gamma_6 Z}{\Gamma_1}(1-Z) \\
& - 4\Gamma_2\Gamma_3\Gamma_5\Gamma_1\Gamma_7 Z^2 - 2\Gamma\Gamma_2\Gamma_4\Gamma_6\Gamma_7\frac{Z}{1-Z} - 4\Gamma\Gamma_2\Gamma_3\Gamma_6\Gamma_7 Z - 2\Gamma_2{}^2\Gamma_6\Gamma_4 \\
& - 4\Gamma_2{}^2\Gamma_6\Gamma_3(1-Z) - \Gamma\Gamma_2\Gamma_4\Gamma_6 - 2\Gamma\Gamma_2\Gamma_3\Gamma_6(1-Z) + \frac{\Gamma\Gamma_2\Gamma_4\Gamma_5\Gamma_6 Z - \Gamma\Gamma_2\Gamma_6{}^2\Gamma_4}{\Gamma_1} \\
& + \frac{2\,\Gamma_2\Gamma\Gamma_5\Gamma_3\Gamma_6 Z - 2\Gamma\Gamma_2\Gamma_6{}^2\Gamma_3}{\Gamma_1}(1-Z) + 4\Gamma_1\Gamma_2\Gamma_3\Gamma_6\Gamma_7 Z - 2\Gamma\Gamma_2\Gamma_5\Gamma_7\frac{Z^2}{1-Z} \\
& - 2\Gamma_2{}^2\Gamma_5 Z - \Gamma\Gamma_2\Gamma_5 Z + \frac{\Gamma_2\Gamma\Gamma_5{}^2\Gamma_4 Z^2}{\Gamma_1} + \frac{2\,\Gamma_2\Gamma\Gamma_5{}^2 Z^2 - 2\Gamma\Gamma_2\Gamma_5\Gamma_6 Z}{\Gamma_1} - 2\Gamma_2\Gamma_5\Gamma_4 Z \\
& + 2\Gamma\Gamma_2\Gamma_6\Gamma_7\frac{Z}{1-Z} + 2\Gamma_2{}^2\Gamma_6 + \Gamma\Gamma_2\Gamma_6 - \frac{\Gamma_2\Gamma\Gamma_6\Gamma_4\Gamma_5}{\Gamma_1} - \frac{\Gamma\Gamma_2\Gamma_6\Gamma_5 Z + \Gamma\Gamma_2\Gamma_6{}^2}{\Gamma_1} \\
& + 2\Gamma_2\Gamma_6\Gamma_4 + 4\Gamma_2\Gamma_3\Gamma_6(1-Z),
\end{aligned}
$$

Received: August 07 2025

Volume 38 No. 5s, 2025

ISSN: 1311-1728 (printed version); ISSN: 1314-8060 (on-line version)

$$D_1 = 2\Gamma_2\Gamma_5\Gamma_4\frac{Z^2}{1-Z} - 4\Gamma_2\Gamma_3\Gamma_5\Gamma\Gamma_7 Z^2 - 2\Gamma_2{}^2\Gamma_4\Gamma_5 Z - 4\Gamma_2{}^2\Gamma_5\Gamma_3 Z(1-Z) - \Gamma\Gamma_2\Gamma_5\Gamma_4 Z$$
$$- 2\Gamma\Gamma_2\Gamma_5\Gamma_3(1-Z) - \frac{\Gamma_2\Gamma\Gamma_6\Gamma_4\Gamma_5 Z}{\Gamma_1} + \frac{4\,\Gamma_2\Gamma\Gamma_5{}^2\Gamma_3 Z^2 - 2\Gamma\Gamma_2\Gamma_5\Gamma_6\Gamma_3}{\Gamma_1}(1-Z)$$
$$+ 4\Gamma_2\Gamma_3\Gamma_5\Gamma_1\Gamma_7 Z - \frac{k\Gamma\Gamma_1{}^2 S_o\Gamma_3}{x_o} + 2\Gamma\Gamma_2\Gamma_6\Gamma_4\Gamma_7\frac{Z}{1-Z} + 4\Gamma_2\Gamma_3\Gamma_6\Gamma\Gamma_7 Z + 2\Gamma_2{}^2\Gamma_4\Gamma_6$$
$$+ 4\Gamma_2{}^2\Gamma_6\Gamma_3(1-Z) + \Gamma\Gamma_2\Gamma_6\Gamma_4 + 2\Gamma\Gamma_2\Gamma_6\Gamma_3(1-Z) + \frac{\Gamma\Gamma_2\Gamma_6{}^2\Gamma_4}{\Gamma_1}$$
$$- \frac{2\,\Gamma_2\Gamma\Gamma_6\Gamma_5\Gamma_3 Z + 2\Gamma\Gamma_6{}^2\Gamma_2\Gamma_3}{\Gamma_1}(1-Z) - 4\Gamma_2\Gamma_3\Gamma_6\Gamma_1\Gamma_7 Z.$$

Therefore, matrix N^1 has four eigenvalues represented by the roots of Eq.(5). Due to Routh-Hurwitz criterion [11] these roots are negative or have negative real parts if the next conditions hold

$$A_1 > 0, C_1 > 0, D_1 > 0, \tag{6}$$

$$(A_1 B_1 - C_1)C_1 - A_1^2 D_1 > 0. \tag{7}$$

Hence, we have the following theorem.

Theorem (1): The point $\in^1$ is locally asymptotically stably of the system of equations (2) when the above requirements (6) and (7) are met.

Analysis of Delayed Model

In theoretical physics, delay time is often used to describe the dynamic behavior of systems. Delay time helps in capturing the transient response of physical systems, allowing a more accurate representation of how systems evolve over time. In the presence of a time delay, the model can become unstable and show more intricate dynamic behaviors, such as Hopf bifurcation and saddle-node behavior. Specially, the features of periodic solutions resulting from the Hopf bifurcation hold great significance,[12]. In actuality, temporal delays occur in a wide range of physical processes, including feedback systems, signal transmission, energy conversion, biological systems, chemical reactions, economic models, and more. Modeling real-world processes is helpful because many real-world processes, such as signal transmission and feedback loops, inherently involve delays. Incorporating delay time into models ensures these processes are accurately represented,[13,14]. Stability analysis with delay times is crucial for analyzing the stability of dynamic systems. Understanding how delays impact system behavior can help prevent oscillations or instability. In control systems or control theory, delay times are factored into the design of controllers to ensure that systems respond optimally, even with inherent delays,[15].

Now model (2) is generalized to assume the following form using the discrete feed delay τ_d.

Received: August 07 2025

International Journal of Applied Mathematics

Volume 38 No. 5s, 2025

ISSN: 1311-1728 (printed version); ISSN: 1314-8060 (on-line version)

$$
\begin{aligned}
\dot{x} &= x(y-1),\\
\dot{y} &= \Gamma z(\Gamma_1 - y)) - \Gamma_2 y(1+2x) - \Gamma_1\Gamma_2,\\
\dot{z} &= \Gamma_1 w(1-z) - \Gamma_2 z - \tfrac{1}{2}\Gamma z\left(1-\tfrac{y}{\Gamma_1}\right),\\
\dot{w} &= \delta_0\,\Gamma_3\left(1-\frac{kx(t-\tau_d)}{x_0}\right) - \Gamma_4 w - 2w(1-z)\Gamma_3.
\end{aligned}
\tag{8}
$$

Where τ_d is the time delay. It is well established that the location and number of equilibrium points remain constant despite time delay. Therefore system (8) still has the interior steady state solution $\in^{\mathbf{1}}$.

Stability Analysis of the Equilibrium $\in^1$ of Model (8)

In the event of a time delay, the stability of model (8) may be effected. So, in this section, we examine the stability $\in^1$ of generalized model (8). Due the presence of time delay τ_d system (8) has a generalized variational matrix that is as follows:

$$
GN(x, y, z, w) = \begin{pmatrix} 0 & x & 0 & 0 \\ -2\Gamma_2 & -\Gamma z - \Gamma_2 - 2\Gamma_2 x & \Gamma(\Gamma_1 - 1) & 0 \\ 0 & \dfrac{\Gamma z}{2\Gamma_1} & -\Gamma w - \Gamma_2 - \dfrac{\Gamma}{2} + \dfrac{\Gamma}{2\Gamma_1} & \Gamma_1(1-z) \\ \dfrac{S_0\Gamma_3 k}{x_0} e^{-\lambda\tau_d} & 0 & 2\Gamma_3 w & -\Gamma_4 - 2\Gamma_3(1-z) \end{pmatrix}
$$

For simplicity GN matrix at $\in^1$ may be written as

$$
GN^1 = \begin{pmatrix} 0 & A^1 & 0 & 0 \\ B^1 & C^1 & D^1 & 0 \\ 0 & E^1 & F^1 & G^1 \\ H^1 e^{-\lambda\tau_d} & 0 & I^1 & J^1 \end{pmatrix},
$$

where,

$A^1 = x^1$, $B^1 = -2\Gamma_2$, $C^1 = -\Gamma z^1 - \Gamma_2 - 2\Gamma_2 x^1$, $D^1 = \Gamma(\Gamma_1 - 1)$, $E^1 = \frac{\Gamma z^1}{2\Gamma_1}$, $F^1 = -\Gamma w^1 - \Gamma_2 - \frac{\Gamma}{2} + \frac{\Gamma}{2\Gamma_1}$, $G^1 = \Gamma_1(1-\mathrm{z})$, $H^1 = \frac{S_0\Gamma_3 k}{x_0}$, $I^1 = 2\Gamma_3 w^1$ and $J^1 = -\Gamma_4 - 2\Gamma_3(1-z^1)$.

Therefore, the system (8) at $\in^1$ has the next characteristic equation

$$
\begin{vmatrix} -\lambda & A^1 & 0 & 0 \\ B^1 & C^1 - \lambda & D^1 & 0 \\ 0 & E^1 & F^1 - \lambda & G^1 \\ H^1 e^{-\lambda\tau_d} & 0 & I^1 & J^1 - \lambda \end{vmatrix} = 0,
$$

it is equivalent to

Received: August 07 2025

International Journal of Applied Mathematics

Volume 38 No. 5s, 2025

ISSN: 1311-1728 (printed version); ISSN: 1314-8060 (on-line version)

$\lambda^4 + A_2\lambda^3 + B_2\lambda^2 + C_2\lambda + D_2 + E_2 e^{-\lambda\tau_d} = 0,$ (9)

Where

$A_2 = -(C^1 + F^1 + J^1),$

$B_2 = C^1F^1 - A^1B^1 - D^1E^1 + C^1J^1 + F^1J^1 - G^1I^1,$

$C_2 = A^1B^1F^1 + A^1B^1J^1 - C^1F^1J^1 + C^1G^1I^1 + D^1E^1J^1,$

$D_2 = A^1B^1G^1I^1 - A^1B^1F^1J^1,$

$E_2 = -A^1D^1G^1H^1.$

First, for $\tau_d = 0$, GN^1 and Eq. (10) reduce to N^1 and Eq. (3) at respectively. Then with the help of theorem (1), still we have $\in^1$ as asymptotically stable point of system (8).

Now, when τ_d has positive value, Eq. (9) may have roots include positive real parts. In this case Eq. (9) must has roots cross the imaginary axis, i.e. it has a pair of pure imaginary roots.

For check this pair of roots, represented by $\lambda = \pm i\sigma, (\sigma > 0)$, exist or not.

If this two values of λ exist, then they must satisfy Eq.(9). Through substituting $\lambda = \sigma i$ in Eq.(8), we derive that

$\sigma^4 - A_2\sigma^3 i - B_2\sigma^2 + C_2\sigma i + D_2 + E_2(\cos(\sigma\tau_d) - i\sin(\sigma\tau_d)\,) = 0.$

This equation has the next real and imaginary part:

$$\begin{aligned} E_2\cos(\sigma\tau_d) &= B_2\sigma^2 - \sigma^4 - D_2, \\ E_2\sin(\sigma\tau_d) &= C_2\sigma - A_2\sigma^3. \end{aligned} \qquad (10)$$

The last equation gives

$$\cos(\sigma\tau_d) = (B_2\sigma^2 - \sigma^4 - D_2)/E_2,$$
$$\sin(\sigma\tau_d) = (C_2\sigma - A_2\sigma^3)/E_2.$$

After squaring $(10)_1$ and $(10)_2$, we may summing the resulting equations to obtain

$\sigma^8 + \hbar_1\sigma^6 + \hbar_2\sigma^4 + \hbar_3\sigma^2 + \hbar_4 = 0,$ (11)

where

$\hbar_1 = {A_2}^2 - 2B_2$, $\hbar_2 = {B_2}^2 + 2D_2 - 2A_2C_2$, $\hbar_3 = {C_2}^2 - 2B_2D_2$, and $\hbar_4 = {D_2}^2 - {E_2}^2$.

Eq.(11) brings us to the subsequent equation after substituting each σ squared with $\bar{\sigma}$ (i.e. $\bar{\sigma} = \sigma^2$).

$\bar{\sigma}^4 + \hbar_1\bar{\sigma}^3 + \hbar_2\bar{\sigma}^2 + \hbar_3\bar{\sigma} + \hbar_4 = 0.$ (12)

Received: August 07 2025

ISSN: 1311-1728 (printed version); ISSN: 1314-8060 (on-line version)

Accordance to Descartes' rule of signs, in the event that $\hbar_1 > 0, \hbar_2 > 0$ and $\hbar_4 < 0$ are fulfilled, there is a unique positive root $\bar{\sigma}$ satisfying Eq. (12). Consequently, $\mp\sigma i$ represents two imaginary roots of Eq. (9).

Therefore, for different values of τ_d, system (2) may establish hopf bifurcation near $\in^1$. Let $\tau_0 = \min\{\tau_d\}$ at which a hopf bifurcation appears. In order to establish that, for $\tau_d = \tau_0$, we need to prove the next condition, denoted the transversality condition,

$$sing\left\{\frac{dRe\lambda(\tau_d)}{d\tau_d}\right\} > 0. \tag{13}$$

To achieve that, assume the root of Equation (9) fulfilling $\rho(\tau_0) = 0$, is $\lambda(\tau_d) = \rho(\tau_d) + i\sigma(\tau_d)$, where $\sigma(\tau_0) = \sigma_0$. Since λ is a function of τ_d, therefore, the differentiation of Equation (9) with regards to τ_d, can be expressed as follows:

$$\left[4\lambda^3 + 3A_2\lambda^2 + 2B_2\lambda + C_2 + E_2\tau_d e^{-\lambda\tau_d}\right]\frac{d\lambda}{d\tau_d} - E_2\lambda e^{-\lambda\tau_d} = 0,$$

and

$$\left(\frac{d\lambda}{d\tau_d}\right)^{-1} = \frac{4\lambda^3+3A_2\lambda^2+2B_2\lambda+C_2}{E_2\lambda}e^{\lambda\tau_d} - \frac{\tau_d}{\lambda}. \tag{14}$$

With $(\tau_d = \tau_0, \lambda = i\sigma_0)$, one can have

$$4\lambda^3 + 3A_2\lambda^2 + 2B_2\lambda + C_2 = (C_2 - 3A_2{\sigma_0}^2) + i(2B_2\sigma_0 - 4{\sigma_0}^3)$$

$$(4\lambda^3 + 3A_2\lambda^2 + 2B_2\lambda + C_2)e^{\lambda\tau_d} =$$

$$= [(C_2 - 3A_2{\sigma_0}^2) + i(2B_2\sigma_0 - 4{\sigma_0}^3)][\cos\sigma_0\tau_0 + i\sin\sigma_0\tau_0]$$

$$= [(C_2 - 3A_2{\sigma_0}^2) + i(2B_2\sigma_0 - 4{\sigma_0}^3)]\left[\frac{B_2{\sigma_0}^2 - {\sigma_0}^4 - D_2}{E_2} + i\frac{C_2\sigma_0 - A_2{\sigma_0}^3}{E_2}\right]$$

$$= \left[(C_2 - 3A_2{\sigma_0}^2)\frac{B_2{\sigma_0}^2 - {\sigma_0}^4 - D_2}{E_2} - (2B_2\sigma_0 - 4{\sigma_0}^3)\frac{C_2\sigma_0 - A_2{\sigma_0}^3}{E_2}\right]$$

$$+i\left[(C_2 - 3A_2{\sigma_0}^2)\frac{C_2\sigma_0 - A_2{\sigma_0}^3}{E_2} + (2B_2\sigma_0 - 4{\sigma_0}^3)\frac{B_2{\sigma_0}^2 - {\sigma_0}^4 - D_2}{E_2}\right],$$

and

$$E_2\lambda = iE_2\sigma_0,$$

further

$$\frac{\tau_d}{\lambda} = -i\frac{\tau_0}{\sigma_0}.$$

Then we have

$$Re\left[\frac{d\lambda}{d\tau_d}\right]^{-1}_{\tau_d=\tau_0}$$

Received: August 07 2025

International Journal of Applied Mathematics

Volume 38 No. 5s, 2025

ISSN: 1311-1728 (printed version); ISSN: 1314-8060 (on-line version)

$$= Re\left[\frac{4\lambda^3 + 3A_2\lambda^2 + 2B_2\lambda + C_2}{E_2\lambda}e^{\lambda\tau_d} - \frac{\tau_d}{\lambda}\right]_{\lambda=i\sigma_0}$$

$$= Re\left[\frac{4\lambda^3 + 3A_2\lambda^2 + 2B_2\lambda + C_2}{E_2\lambda}e^{\lambda\tau_d}\right]_{\lambda=i\sigma_0}$$

$$= \frac{1}{E_2\sigma_0}\left[(C_2 - 3A_2{\sigma_0}^2)\frac{C_2\sigma_0 - A_2{\sigma_0}^3}{E_2} + (2B_2\sigma_0 - 4{\sigma_0}^3)\frac{B_2{\sigma_0}^2 - {\sigma_0}^4 - D_2}{E_2}\right]$$

$$= \frac{1}{{E_2}^2}[(C_2 - 3A_2{\sigma_0}^2)(C_2 - A_2{\sigma_0}^2) + (2B_2 - 4{\sigma_0}^2)(B_2{\sigma_0}^2 - {\sigma_0}^4 - D_2)]$$

$$= \frac{1}{{E_2}^2}\left[4{\sigma_0}^6 + \left(3{A_2}^2 - 6B_2\right){\sigma_0}^4 + \left(2{B_2}^2 - 4A_2C_2 + 4D_2\right){\sigma_0}^2 - 2B_2D_2 + {C_2}^2\right]$$

$$= \frac{1}{{E_2}^2}[4{\sigma_0}^6 + 3\hbar_1{\sigma_0}^4 + 2\hbar_2{\sigma_0}^2 + \hbar_3]$$

$$= \frac{1}{{E_2}^2}\bar{\hbar}({\sigma_0}^2),$$

where,

$\bar{\hbar}({\sigma_0}^2) = 4{\sigma_0}^6 + 3\hbar_1{\sigma_0}^4 + 2\hbar_2{\sigma_0}^2 + \hbar_3.$

Let $\varkappa = {\sigma_0}^2 > 0$, then one can show that from complex analysis

$$sing\left[\frac{d(Re\,\lambda(\tau_d))}{d\tau_d}\right]^{-1}_{\tau_d=\tau_0} = sing\;Re\left[\frac{d\lambda(\tau_d)}{d\tau_d}\right]^{-1}_{\tau_d=\tau_0} = sing\left[\bar{\hbar}(\varkappa)\right].$$

Clear we have $\bar{\hbar}'(\varkappa) = 12\varkappa^2 + 6\hbar_1\varkappa + 2\hbar_2 > 0$. So that in $[0,\infty]$, $\bar{\hbar}(\varkappa)$ is monotonously increases.

Furthermore, with the condition

$${B_2}^2 + 2D_2 > 2A_2C_2. \qquad (15)$$

On can get $\bar{h}(0) > 0$, and $\bar{h}(\varkappa) > 0$ for $\sigma > 0$.

Consequently, the transversal condition (13) is satisfy if condition (15) is met.

Theorem (2): Assume that the condition (15) holds, then when $\tau_d \in [0; \tau_0)$ all roots of equation (9) have negative real parts, and when $\tau_d = \tau_0$ equation (9) has a pair of purely imaginary roots $\pm i\sigma$ while all other roots have negative real parts.

Numerical analysis

Received: August 07 2025

Volume 38 No. 5s, 2025

ISSN: 1311-1728 (printed version); ISSN: 1314-8060 (on-line version)

In this section to reveal the systems fascinating complicated behavior, the numerical simulations of QDL model (2) are run using the Matlab software to illustrate the analytical results. In this simulation we used the hypothetical collection of data.

Table (1): Parameters used in our numerical simulation of QDL model (8)[16].

Parameters	Value
Γ	8.12403
Γ_1	1.78819
Γ_2	0.07
Γ_3	5.32
Γ_4	0.0366222
$\delta_\circ$	0.095
k	0.75
x_0	2

First, in order to investigate the impact of varying parameters on the dynamical behavior of model of QDL (5), the following results are observed.

Received: August 07 2025

International Journal of Applied Mathematics

Volume 38 No. 5s, 2025

ISSN: 1311-1728 (printed version); ISSN: 1314-8060 (on-line version)

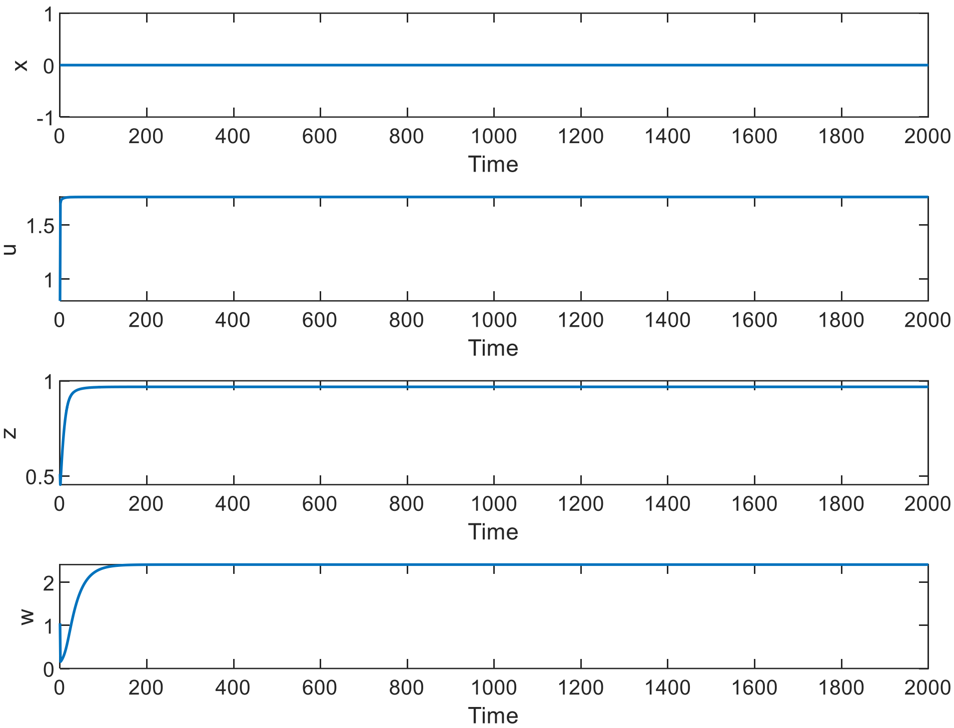

Figure(1): The time series for the QDL model (2) with parameter values as in table (1) with $\delta_\circ = 0.1$. The trajectories converge to the boundary equilibrium $\in^{\circ} = (0\,,\ 1.7566,\ 0.9682,\ 2.4112)$.

The numerical result shows that $B = -643.0020 < 0$, therefore, the condition for the QDL model (2) to have a boundary fixed point is met, as shown in Fig. 1 which refers to the steady state for all layers.

Figure (2), with the data set in table (1), shows that the trajectories of QDL model (2) converge to interior equilibrium $\in^{1} = (0.3857 \quad 1.0000 \quad 0.0389 \quad 0.0421)$. In this figure the time series of the behaviors of x, u, z and w shows that the dynamic of model (2) is locally asymptotically stabile near $\in^{1}$. The numerical result show that the interior fixed point exists where $B = -397.5058 < 0$, and it is asymptotically stabile as plotted in Fig.(2). It is noted that the effect was limited to the moment of operation, and then the behavior stabilized around the equilibrium points.

Received: August 07 2025

International Journal of Applied Mathematics

Volume 38 No. 5s, 2025

ISSN: 1311-1728 (printed version); ISSN: 1314-8060 (on-line version)

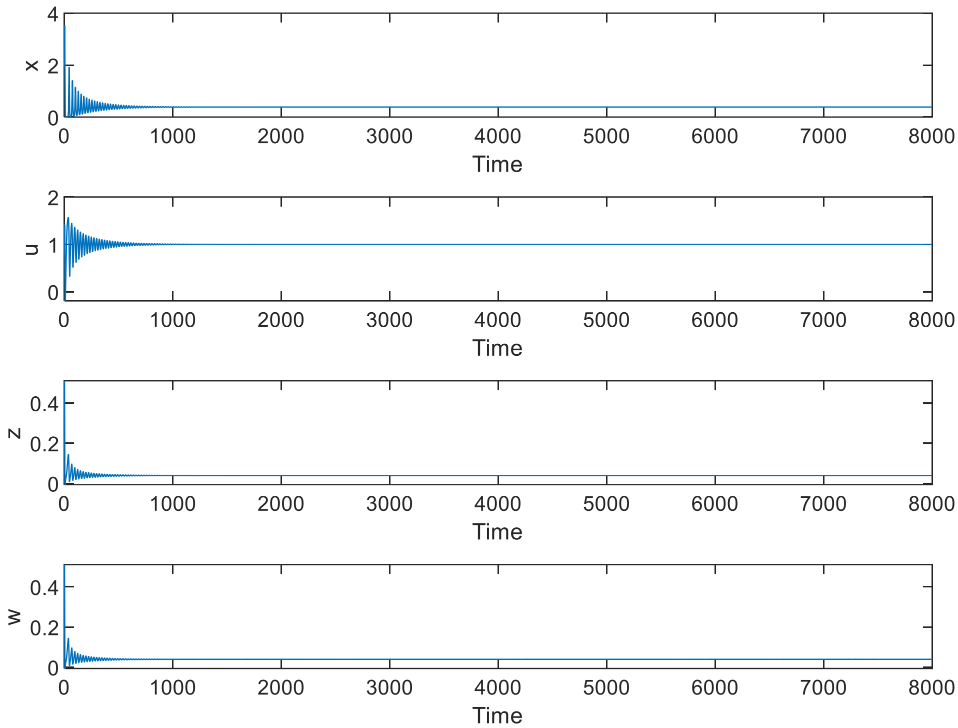

Figure (2): The time series for the QDL model (2) where the trajectories converge to the interior equilibrium $\in^1 =$ $(0.3857 \quad 1.0000 \quad 0.0389 \quad 0.0421)$.

Studying how delayed time affects the dynamics of semiconductor lasers is essential for both fundamental science and advanced optical technologies. In other hand, to explore the effect of time delay on the QDL model (8) with $\tau_d \leq 3$ and others parameters values as given in set (1) is plotted in figs. 2 and 3. In these figures the dynamic of QDL model (8) still converges to interior fixed point $\in^1 = (0.3857 \quad 1.0000 \quad 0.0389 \quad 0.0421$, and the numerical result show that $h_1 = 153.6$, $h_2 = 4816.2$, $h_3 = 79.6$, and $h_4 = 13.0$. This means the equation (11) can't has any positive root and the first condition to appear Hopf bifurcation not satisfied.

To explore the effect of increasing the time delay the numerical summation of QDL model (8) at $\tau_d = 4$ is presented in figs. 4 and 5. These figures show that the stability of interior fixed point $\in^1$ lost where the system (8) undergoes a Hopf bifurcation and the trajectories converges to limit cycle.

In Figs. 6 and 7 the numerical summation of QDL model (8) at $\tau_d = 4$ with $\mathrm{k} = 1.2$ is presented. These figures also show that the system (8) undergoes a Hopf bifurcation and the trajectories converges faster to limit cycle. Same behavior of system (8) can be obtain by increasing the value of $\delta_\circ$, see Fig. 8 for $\delta_\circ = 0.12$. The effect of time delay can be reduced through by decreasing the value of parameter k as see in fig. 9. In this figure $\mathrm{k} = 0.5$ the system settles converges to interior fixed point $\in^1$. Same result's of Fig, 9 can be obtain by decreasing the value of parameter $\delta_\circ$ as shown in Fig. 10 at $\delta_\circ = 0.09$. The increasing of the time-delayed

Received: August 07 2025

International Journal of Applied Mathematics

Volume 38 No. 5s, 2025

ISSN: 1311-1728 (printed version); ISSN: 1314-8060 (on-line version)

feedback induces chaos in semiconductor lasers. This is crucial for applications like secure optical communications, where chaos is used to mask signals.

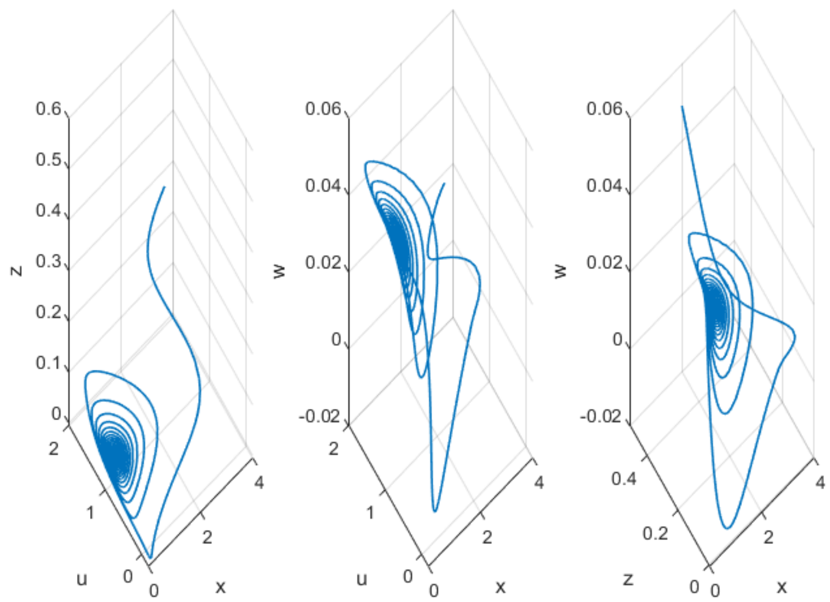

Figure (3): Phase portrait for the QDL model (8) with data in Table 1 and $\tau_{d=}3$, show the stability of the interior fixed point $\in^1$.

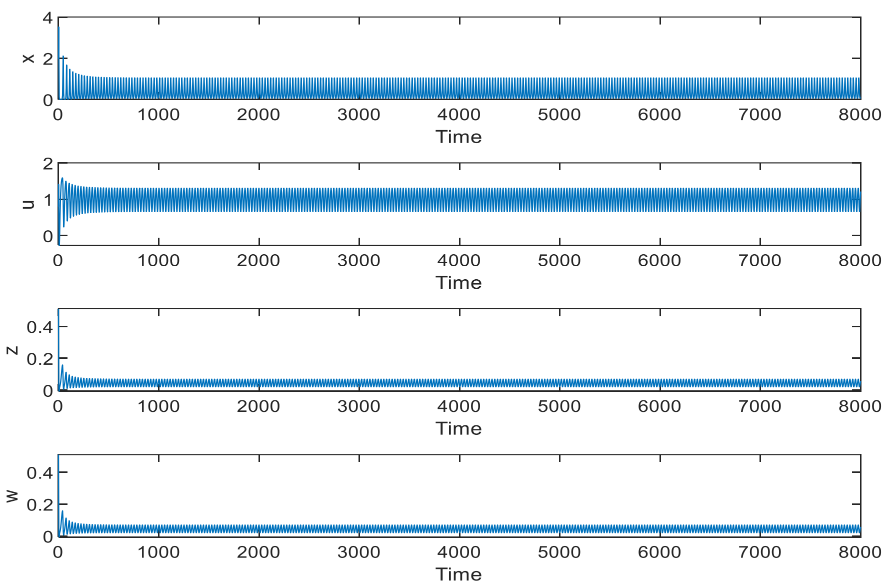

Figure (4): The time series of QDL model (8) with data in Table 1 and $\tau_{d=}4$, show instable the interior fixed point $\in^1$.

Received: August 07 2025

International Journal of Applied Mathematics

Volume 38 No. 5s, 2025

ISSN: 1311-1728 (printed version); ISSN: 1314-8060 (on-line version)

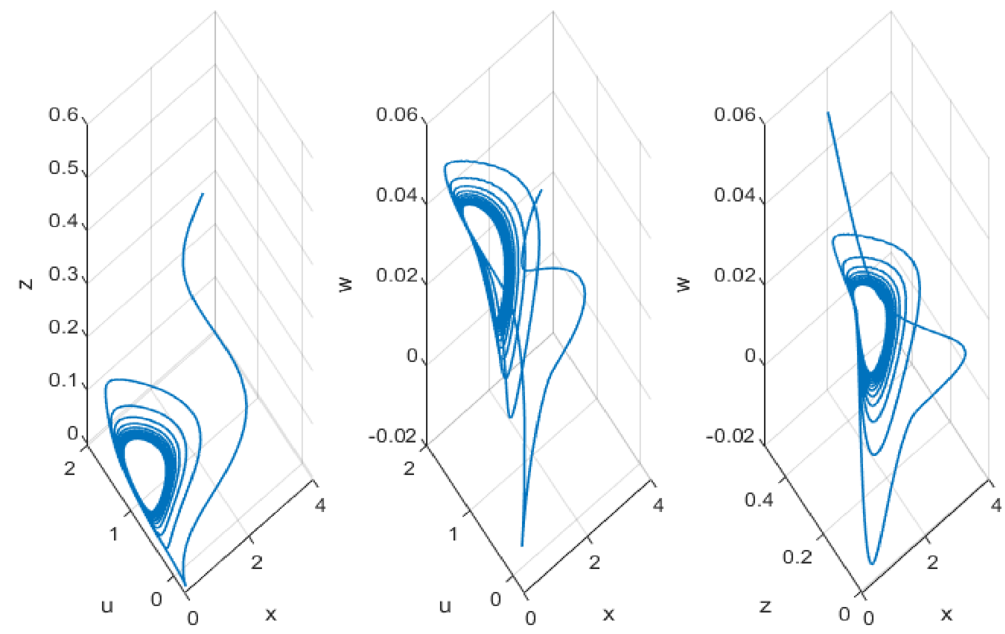

Figure (5): Phase portrait for the QDL model (8) with data in Table 1 and $\tau_{d=}4$, show instable the interior fixed point $\in^1$.

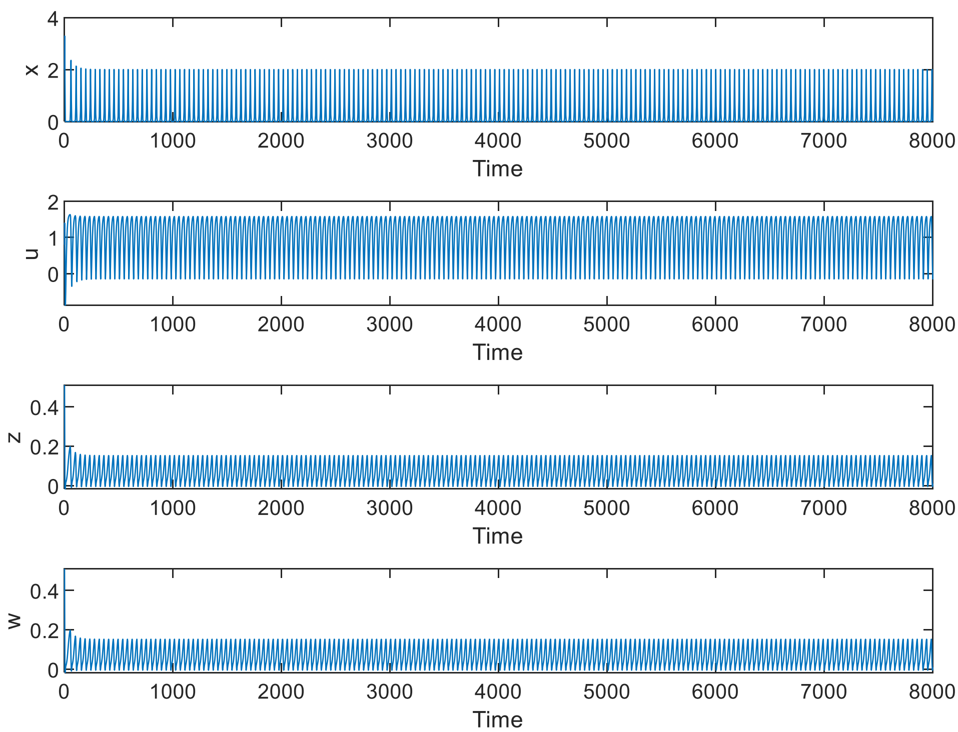

Received: August 07 2025

International Journal of Applied Mathematics

Volume 38 No. 5s, 2025

ISSN: 1311-1728 (printed version); ISSN: 1314-8060 (on-line version)

Figure (6): The time series of QDL model (8) with $k = 1.2$ and $\tau_{d=}4$, show instable the interior fixed point $\in^1$.

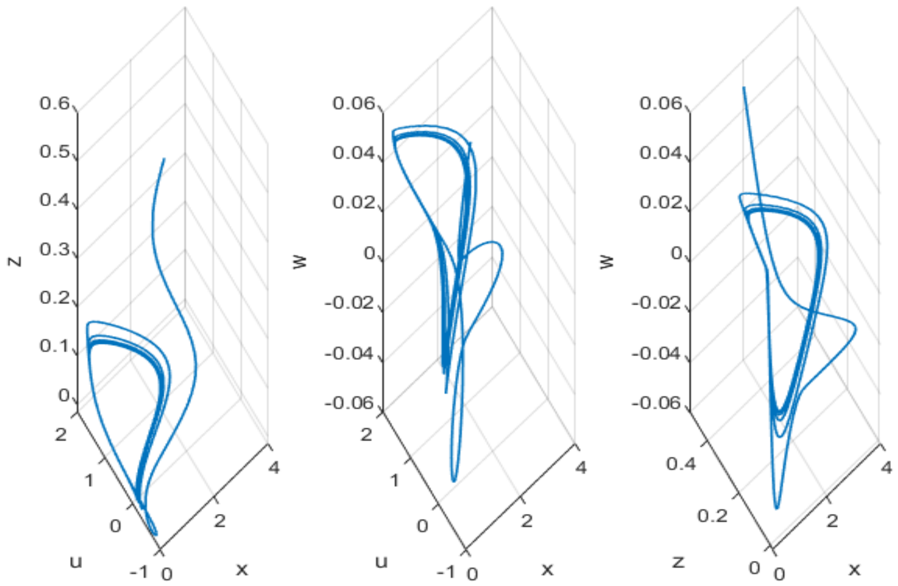

Figure (7): Phase portrait for the QDL model (8) with $k = 1.2$ and $\tau_{d=}4$, show instable the interior fixed point $\in^1$.

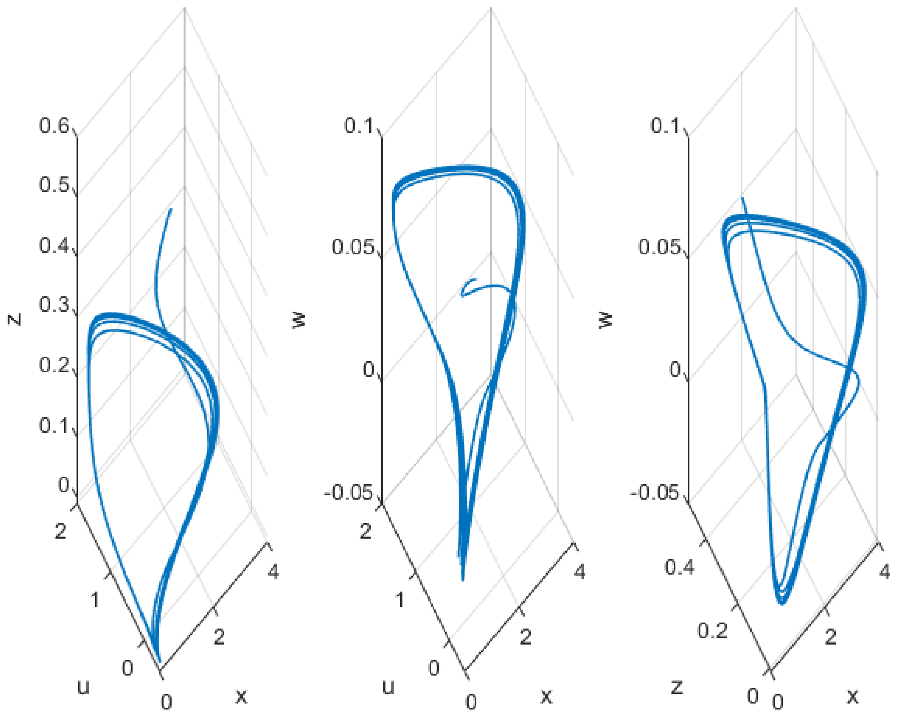

Received: August 07 2025

International Journal of Applied Mathematics

Volume 38 No. 5s, 2025

ISSN: 1311-1728 (printed version); ISSN: 1314-8060 (on-line version)

Figure (8): Phase portrait for the QDL model (8) with $\delta_{\circ} = 0.12$ and $\tau_{d=}4$, show instable the interior fixed point $\in^1$.

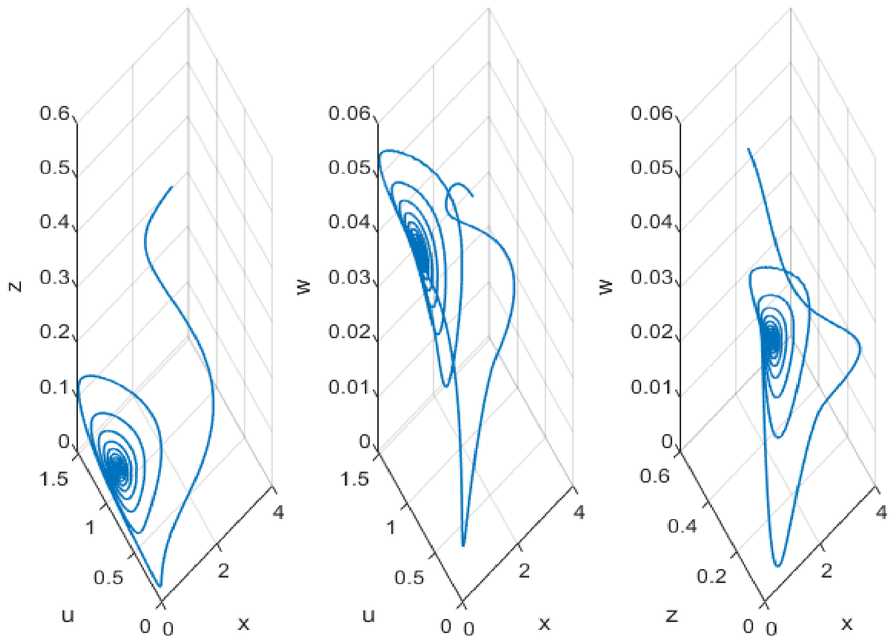

Figure (9): Phase portrait for the QDL model (8) with $\mathrm{k} = 0.5$ and $\tau_{d=}4$, show stable the interior fixed point $\in^1$.

Received: August 07 2025

International Journal of Applied Mathematics

Volume 38 No. 5s, 2025

ISSN: 1311-1728 (printed version); ISSN: 1314-8060 (on-line version)

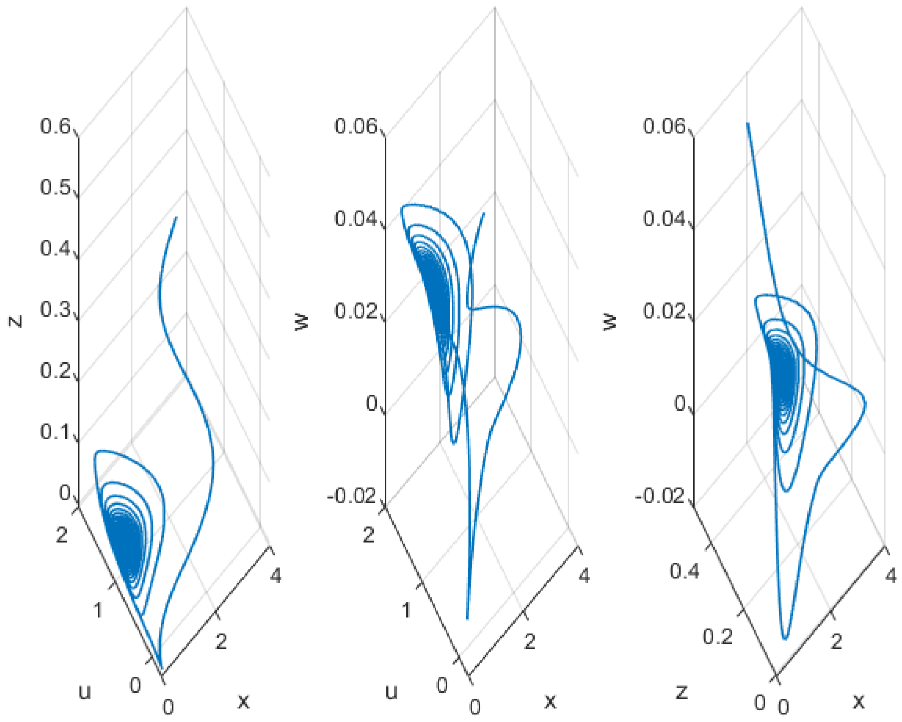

Figure (10): Phase portrait for the QDL model (8) with $\delta_{\circ} = 0.09$ and $\tau_d = 4$, show stable the interior fixed point $\in^1$.

Conclusion

A theoretical study has been done on the chaotic behavior dynamics of semiconductor lasers with OEFB. In this investigation, the following conclusions can be drawn. Mathematical model was proposed for the work of the QD laser system, which consists of four equations that were chosen from a mathematical QDL model. Also, after a series of mathematical operations, these equations were converted into dimensionless equations. On the analytical side, the following was observed:

- If the values of $(k, \delta_{\circ})$ are positive, the model contains two equilibrium points, one of which is the boundary point $\in^{\circ}$ when (x = 0), and the other is the interior point $\in^1$ when (u = 1). Further, $\in^1$exists if z take the values in the range ($0 < z < 1$).
- The stability of the system at the interior point $\in^1$ is discussed, and we found the solutions (x, u, z, w) approach asymptotically to the values of point $\in^1$, when the conditions $A_1 > 0, C_1 > 0, D_1 > 0, (A_1B_1 - C_1)C_1 - A_1^2D_1 > 0$ are met..

Received: August 07 2025

- The quantum dot laser model was generalized by adding the delay time, and the generalized system also contains one internal point $\in^1$.
- In the generalized model, we found that the stability of the point $\in^1$ is affected by the value of τ_d, as when the value of $\tau_d \leq 3$, the generalized system still converge to the point $\in^1$. Further, when the value of $\tau_d \geq 3$ and the other parameters as given in table 1, loses its stability and the solutions for the variables (x,u,z,w) move away from the point and take periodic paths, and the system has a bifurcation of a Hopf type or a limit cycle affected by the value of τ_d.

Conflicts of interest. The authors declare that they have no conflict of interest.

Author contributions. All the authors contributed equally in this work.

Data Availability Statement. Data are analyzed and included in this manuscript. The detailed data could be shared with the corresponded author upon a reasonable request.

Reference

[1] Al Attabi, T.A., Al Husseini, H.B. "Equilibrium points, linear stability, and bifurcation analysis on the dynamics of a quantum dot light emitting diode system" Journal of Optical Communications, 2025, 46(1), pp. 93–105

[2] Mahdi, A.S., Al Husseini, H.B." Filtered optical feedback modes effect on quantum-dot laser behavior"Journal of Optics (India), 2024, 53(3), pp. 1972–1983

[3] Kareem, Z.S., Husseini, H.B.A." Study of the Dynamic Properties of Chaotic Circuits in the Presence of Memristors" International Journal of Thin Film Science and Technology, 2024, 13(2), pp. 153–168

[4] Mahdi, A.S., Al Husseini, H.B."Quantum dot laser dynamics and external filtered modes under the influence of double-filtered optical feedback"Physica Scripta, 2024, 99(4), 045108

[5] Ali, H.M., Al Husseini, H.B."Synchronization of chaotic network quantum dot light-emitting diodes under optical feedback" Journal of Optics (India), 2020, 49(4), pp. 573–579

[6] F. Rogister, A. Locquet, D. Pieroux, M. Sciamanna, O. Deparis, P. Megret, and M. Blondel, ºSecure communication scheme using chaotic laser diodes subject to incoherent optical feedback and incoherent optical injection,º Opt. Lett., vol. 26, pp. 1486-1488, (2001).

[7] J. M. Saucedo Solorio, D. W. Sukow, D. R. Hicks, and A. Gavrielides, ºBifurcations in a semiconductor laser subject to delayed incoherent feedback,º Opt. Commun., vol. 214, pp. 327-334, (2002).

[8] May R.M., Stability and complexity in model ecosystem., Princeton, New Jersey: Princeton University Press, (1973). [9] Sabharwal, Rohit. Introduction to System Dynamics. Educohack Press, (2025).

[10] W.K.Irhaif and H.B. Al Husseini, "Stability Analysis and Bifurcation in External Cavity Quantum Dot Semiconductor Laser", 2nd International Scientific Conference of Al-Ayen

Received: August 07 2025

Volume 38 No. 5s, 2025
ISSN: 1311-1728 (printed version); ISSN: 1314-8060 (on-line version)

University (ISCAU-2020). IOP Conf. Series: Materials Science and Engineering 928, 072042, doi:10.1088/1757-899X/928/7/072042, (2020).

[11] May R.M., Stability and complexity in model ecosystem., Princeton, New Jersey: Princeton University Press, (1973).

[12] Sabharwal, Rohit. Introduction to System Dynamics. Educohack Press, (2025).

[13] E. Buraimoh, G. Ozkan,L. Timilsina, P. K. Chamarthi, B. Papari, C. S. Edrington. "Overview of interface algorithms, interface signals, communication and delay in real-time co-simulation of distributed power systems." IEEE Access 11: 103925-103955, (2023).

[14] Nilsson, Johan. "Real-time control systems with delays." PhD Thesis TFRT-1049 (1998).

[15] Rionero, S. Hopf bifurcations in dynamical systems. Ricerche mat 68, 811–840 (2019).

[16]S.A.AlJabri1and H. B. Al Husseini," Effect of phase conjugate coupled on routes to chaos in incoherent optical feedback semiconductor quantum dot laser" J Opt, The Optical Society of India. https://doi.org/10.1007/s12596-022-00894-0, (2022).

Received: August 07 2025